scientific reports

Check for updates

OPEN

Symptomatic and pathological features in chemical phlebitis rat model by injection vinorelbine via dorsal pedal vein

Haijie Ji[1,4], Xudong Shi[2,4], Shumin Wang[1], Shu Wang[1], Dongxue Yan[1], Liguo Tong[1], Qiming Zhong[1], Mali Feng[1], Shulan Hao[1], Weiping Li[3]✉ & Xixing Wang[1]✉

Intravenous administration of vesicants or irritants frequently leads to chemical phlebitis. We aimed to establish a chemical phlebitis rat model by injection vinorelbine via dorsal pedal vein and evaluate the general symptoms as well as the pathological features of lesion venous tissues. Rats in 6 groups with each 8 were injected 0.1 mL saline or vinorelbine (1–5 mg/mL) via the dorsalis pedis vein in hind paw, respectively. The edema and pain were assessed daily by swelling rates (water displacement) and weight-bearing ratio (bipedal balance test), respectively. Phlebitis severity was evaluated by phlebitis scale. Venous tissues harvested on day 7 were underwent histopathological and ultrastructural evaluation. Vinorelbine administration elicited dose-dependent inflammatory responses, with erythema, edema, pain, palpable cord formation, and purulent drainage. Edema and pain peaked on day 3, as evidenced by increased swelling rates and reduced weight-bearing ratios. Persistent symptomatology was observed in the 3–5 mg/mL groups through day 7. Histopathological analysis demonstrated venous wall thickening characterized by intimal hyperplasia and collagen deposition, along with vascular lumen stenosis accompanied by thrombosis. Furthermore, disruption of the intimal lining was observed, with shrunken endothelial cells interspersed among extracellular matrix. These pathological changes also exhibited a dose-dependent exacerbation with increasing concentrations of vinorelbine. Dorsal pedal vein injection of 0.1 mL vinorelbine (3–5 mg/mL) successfully induced chemical phlebitis in rats, mimicking human clinical presentations. Furthermore, vinorelbine-induced endothelial damage resulted in distinct venous lesions, characterized by vascular wall thickening with intimal hyperplasia, luminal stenosis and thrombus.

Keywords Rat model, Chemical phlebitis, Symptomatic features, Venous pathology, Vinorelbine, Dorsal pedal vein

Intravenous chemotherapy is a cornerstone treatment in modern medicine. However, administration of vesicants[1] or irritants[2] often leads to a local venous inflammation with manifestations including erythema, pain, edema, increased warmth, palpable cord, and purulent drainage, namely chemical phlebitis[3,4]. These symptoms may persist for months, which profoundly impact patients' quality of life and normal daily activities[5]. Despite advances in preventive strategies[6], chemical phlebitis remains a prevalent complication, particularly among pediatric[7] and malignant tumor patients[8]. Therefore, it is necessary to explore the pathophysiological features of chemical phlebitis using experimental animal models, which may help raise awareness of its harm.

Current animal models of chemical phlebitis primarily rely on intravascular injection, for rabbits via the marginal ear vein[9–13] and mice via the lateral tail vein[14,15], which is more for the former. However, these models present several anatomical and practical limitations. The rabbit auricle is composed primarily of thin skin and cartilage tissue, with the marginal ear vein being superficial yet highly branched, featuring numerous collateral vessels. Similarly, the mouse tail is covered by circular keratin scales and dense collagen, where the lateral tail vein is both fine and deeply positioned, rendering intravenous injections technically challenging. Crucially, both the auricle and tail lack substantial soft tissue components such as muscle and adipose tissue. As a result, animal models utilizing these sites fail to fully replicate the clinical manifestations of chemical phlebitis. Additionally, it

[1]Shanxi Province Academy of Traditional Chinese Medicine, Taiyuan 030012, China. [2]North University of China, Taiyuan 030051, China. [3]Fenyang College, Shanxi Medical University, Fenyang 032200, China. [4]Haijie Ji and Xudong Shi have contributed equally to this work. ✉email: liweiping0929@163.com; wangxx315@163.com

is difficult to sample lesioned vein specimens from these sites for histological studies, particularly for examining tunica intima microstructure and endothelial cell morphology.

In this study, a rat model of chemical phlebitis was established by intravascular administration of vinorelbine solution in a concentration-gradient manner via the dorsalis pedis vein of the hindpaw. The severity of phlebitis was evaluated using a standardized phlebitis scale, which assessed clinical indicators including erythema, pain, edema, palpable cord formation, and purulent drainage. Furthermore, pathological featues of venous tissues was observed by hematoxylin-eosin and masson's trichrome staining, as well as scanning and transmission electron microscopy.

Materials and methods

Animals

A total of 48 male Sprague-Dawley rats (9 weeks old, 300 ~ 320 g) were acquired from Beijing HFK Bioscience Co., Ltd (China) and housed in a temperature-controlled room (22 ~ 24 °C) with a 12/12 light/dark cycle and fed with standard rat chow and tap water. All procedures were approved by the Medical Ethics Committee of the Shanxi Academy of Traditional Chinese Medicine (Approval Number: SZYLY2022KY-0302). All experiments were performed in accordance with relevant guidelines and regulations, and the authors complied with the ARRIVE guidelines.

Modeling method

The rats were randomly divided into 6 groups, with each 8 in each group. The right hindlimb hair was removed by depilatory cream 1 day earlier. Then the rat was anesthetized with 2% isoflurane and the right knee was wrapped by a rubber tourniquet to engorge the dorsalis pedis vein for easy puncture. The chemical phlebitis was induced in rats of 5 groups by injecting 0.1 mL of 1 mg/ mL, 2 mg/mL, 3 mg/mL, 4 mg/mL, and 5 mg/mL vinorelbine solution, respectively. While the remaining rats were received 0.1 mL of normal saline serving as sham group. The puncture site was pressed for 5 min to prevent bleeding or drug leakage after injection. Then the general symptoms of phlebitis were observed daily. On day 7, the animals were euthanized with Euthasol (100 mg/kg, IV), and a 1-cm segment of the vein extending proximally from the puncture site in the right hindlimb was collected for histopathological examination.

Hindlimb volume test

The volume of the injected hindlimb (2 cm above the ankle) in rat was measured by drainage method[16] before modeling and post-model daily for 7 days. The edema was quantified as swelling rate, which is calculated by the following formula:

$$\text{Swelling rate } (\%) = \frac{\text{Post - model volume} - \text{initial volume}}{\text{Initial volume}} \times 100\%$$

Bipedal balance test

Pain was evaluated by weight-bearing ratio of treated hindlimb, which is determined by the bipedal balance test[17] before modeling and post-model daily for 7 days. Briefly, the rats were placed in the bipedal balance analgesiometer and make sure both of the hind paws stand on the corresponding pressure sensors for recording the bilateral paw pressures, respectively. The weight-bearing ratio is calculated by the following formula:

$$\text{Weight - bearing ratio } (\%) = \frac{\text{Pressure on the injected paw}}{\text{Total pressure of both paws}} \times 100\%$$

Phlebitis grading

The symptoms of chemical phlebitis including erythema, pain, edema, palpable cord, and purulent drainage in the injected hindlimb were observed each day for 7 and the severity was graded according to the phlebitis scale[18] shown in Table 1.

Grade	Description
0	No symptoms
I	Erythema at or near site, with or without pain
II	Erythema and/or swelling at site, with pain
III	Erythema and/or swelling, pain, induration and streak formation
IV	Erythema and/or swelling, pain, induration, streak formation, purulent drainage

Table 1. Phlebitis grading scale.

Hematoxylin-eosin and masson's trichrome staining

The venous tissues were fixed in 4% polyformaldehyde, dehydrated and embedded in paraffin blocks. Subsequently, transverse sections of 5 μm were stained with hematoxylin-eosin (HE) and masson's trichrome staining, respectively. Images were visualized using an M8 digital scanning microscopy imaging system (Lecia).

Electron microscopy

The venous tissues were pre-fixed with 3% glutaraldehyde at 4 °C for 2 days and post-fixed with 1% osmic acid for 2 h. Subsequently, the tissues were gradually dehydrated with 50–100% ethanol. For scanning electron microscopy (SEM), the longitudinal section of veins was treated by isoamyl acetate for 15 min and dried by a critical point dryer. Specimens were attached to metallic stubs by carbon stickers and sputter-coated with gold for 30 s. Then the sections were observed and captured by SEM (HITACH, SU8100). For transmission electron microscopy (TEM), transverse sections of veins were immered in 100% acetone/Epon 812 and ultrathin slices (60 nm) were prepared. The sections were stained with 5% uranium acetate for 30–60 min and then with lead citrate for 10 min. After drying, the sections were observed and captured by TEM (HITACH, HT7800).

Statistical analysis

The data were analyzed using the SPSS software version 22.0. The swelling rate and weight-bearing ratio were presented as mean ± standard deviation. Comparisons between the two groups were conducted using the independent *t*-test. The Kruskal-Wallis one-way analysis of variance was used to analyze the grading of phlebitis. A *p*-value of less than 0.05 was considered statistically significant.

Results

General symptoms in hindlimbs

The general symptoms in hindlimb of rats following intravenous injection of saline or vinorelbine via the dorsal pedal vein were observed daily for 7 days. Representative photographs were captured every other day, as depicted in Fig. 1. During observation period, sham-operated rats (0 mg/mL) exhibited no signs of erythema or edema in the hindlimb with skin intact. In contrast, rats administered vinorelbine displayed marked erythema and edema

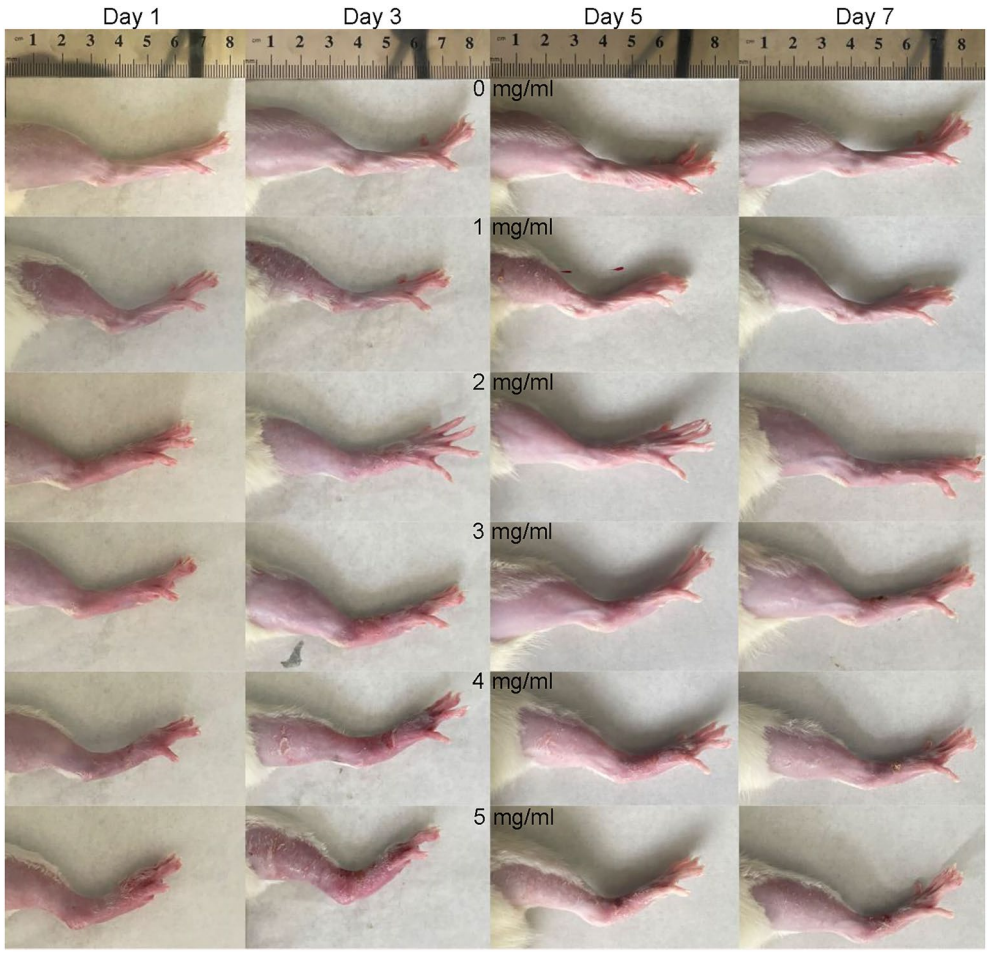


Fig. 1. The general symptoms of injected hindlimb in rats induced by different concentrations of vinorelbine via dorsal pedal vein, with images taken every other day.

Group mg/ml	Dose mg/kg	1 d	3 d	5 d	7 d
0	0	-1.71 ± 2.31	0.94 ± 0.78	1.97 ± 1.52	-0.82 ± 0.68
1	0.32	8.37 ± 3.53*	2.11 ± 1.42	1.93 ± 0.24	-0.62 ± 0.75
2	0.65	19.13 ± 6.24***	29.60 ± 5.81***	15.43 ± 5.63***	6.12 ± 3.41*
3	0.94	36.59 ± 7.36***	63.14 ± 9.75***	43.17 ± 11.27***	33.45 ± 13.04***
4	1.25	61.89 ± 12.93***	85.37 ± 17.65***	68.52 ± 13.46***	51.82 ± 9.63***
5	1.56	93.18 ± 15.62***	128.31 ± 23.49***	102.16 ± 19.81***	86.96 ± 12.51***

Table 2. Comparison of swelling rates induced by different concentration of vinorelbine. Data are expressed as the mean ± standard deviation (SD). Compared with 0 mg/mL group, $^{**}p < 0.01$,$^{***}p < 0.001$.

Group mg/ml	Dose mg/kg	1 d	3 d	5 d	7 d
0	0	50.0 ± 1.2	49.8 ± 1.4	50.1 ± 3.2	50.4 ± 2.1
1	0.32	50.6 ± 1.4	48.3 ± 2.6	50.3 ± 2.9	50.7 ± 1.3
2	0.65	50.1 ± 2.1	45.1 ± 2.9**	46.8 ± 2.7**	48.5 ± 2.8
3	0.94	49.2 ± 3.6	40.5 ± 3.7***	42.9 ± 3.0***	46.7 ± 2.5**
4	1.25	48.6 ± 2.7	33.8 ± 1.9***	37.8 ± 2.4***	43.6 ± 2.3***
5	1.56	47.3 ± 2.1	30.2 ± 2.3***	35.8 ± 3.1***	41.5 ± 3.7***

Table 3. The weight-bearing ratio of the injected hindlimb in rats. Data are expressed as the mean ± standard deviation (SD). Compared with 0 mg/mL group, $^{**}p < 0.01$, $^{***}p < 0.001$.

as early as day 1 post-injection, with symptom severity escalating in a dose-dependent manner. By day 3, these manifestations progressed, accompanied by ulcer formation. Subsequently, partial alleviation of erythema and edema was observed by day 5. However, these improvements were followed by the development of induration and streak formation by day 7.

Edema evaluation

As illustrated in Table 2, the swelling rate of hindlimb in rats treated by all concentration of vinorelbine significantly increased compared to the sham rats on the 1st day post-injection. Furthermore, the swelling rate increased in accordance with the ascending concentration of vinorelbine solution and the peak was observed on the 3rd day. After that, the swelling rate exhibited a slight decrease on the 5th day but still remained above 30% in the 3 mg/mL, 4 mg/mL and 5 mg/mL vinorelbine groups on the 7th day.

Pain evaluation

Pain was identified when the weight-bearing ratio of injected paw in bipedal stance testing fell below 50%. As shown in Table 3, the weight-bearing ratio of injected paw in sham group maintained about 50% during the experimental period. In contrast, the ratio in rats injected with vinorelbine solution may less than 50%, the extent of which depended on the timepoint and vinorelbine concentration. On the 1st day, the ratio in rats of all vinorelbine-treated groups with a slight decrease tendecy was observed compared to the sham rats. Obviously, the ratio was decreased markly on the 3rd and 5th day, especially in the 3 mg/mL, 4 mg/mL and 5 mg/mL vinorelbine groups. By the end of day 7, the ratio of injected paw in rats treated by 4 mg/mL and 5 mg/mL vinorelbine still significantly decreased compared to the sham rats.

Grading of chemical phlebitis by phlebitis scale

The chemical phlebitis in each rat was graded by phlebitis scale on day 7 and the results were shown in Table 4. The severity of chemical phlebitis among these groups was correlated with the concentration of vinorelbine solution. All the rats in sham group (0 mg/mL) and 1 mg/mL vinorelbine group were graded 0 with no symptoms. While in the 2 mg/mL vinorelbine group, 37.5% of the rats were graded 0 and 62.5% displayed grade I. The incidence of grade I, II and III in the 3 mg/mL group were 25%, 50% and 25%, respectively. In the 4 mg/mL group, the incidence of grade II, III, and IV were 25%, 50% and 25%, respectively. The grade III and IV account for 37.5% and 62.5% in the 5 mg/mL group, respectively.

Hispathological features in venous tissues

Hematoxylin-eosin staining was performed on venous tissues sampled from the injected hindlimb of rats on day 7 with representative graphs shown in Fig. 2. Venous tissues from 0 mg/mL exhibited normal morphology, characterized by flexible vessel walls with classical layers of tunica adventitia, media and intima. The intima displayed hobnailed endothelium and the lumen was free of thrombus. Veins from rats treated with 1 mg/mL vinorelbine showed nearly identical histological features to normal veins, with no significant pathological alterations. However, the thicken vein wall were presented in the venous tissues collected from the rats injected 2 mg/mL vinorelbine. More pronounced pathological changes were observed in the 3, 4, and 5 mg/mL vinorelbine

Group mg/ml	Dose mg/kg	Grade					P
		0	I	II	III	IV	
0	0	8 (100.0%)	0 (0.0%)	0 (0.0%)	0 (0.0%)	0 (0.0%)	-
1	0.32	8 (100.0%)	0 (0.0%)	0 (0.0%)	0 (0.0%)	0 (0.0%)	1.000
2	0.65	3 (37.5%)	5 (62.5%)	0 (0.0%)	0 (0.0%)	0 (0.0%)	0.023*
3	0.94	0 (0.0%)	2 (25.0%)	4 (50.0%)	2 (25.0%)	0 (0.0%)	< 0.001***
4	1.25	0 (0.0%)	0 (0.0%)	2 (25.0%)	4 (50.0%)	2 (25.0%)	< 0.001***
5	1.56	0 (0.0%)	0 (0.0%)	0 (0.0%)	3 (37.5%)	5 (62.5%)	< 0.001***

Table 4. The grading of chemical phlebitis assessed by phlebitis scale on day 7. Compared with 0 mg/mL group, $^{*}p < 0.05$, $^{***}p < 0.001$.

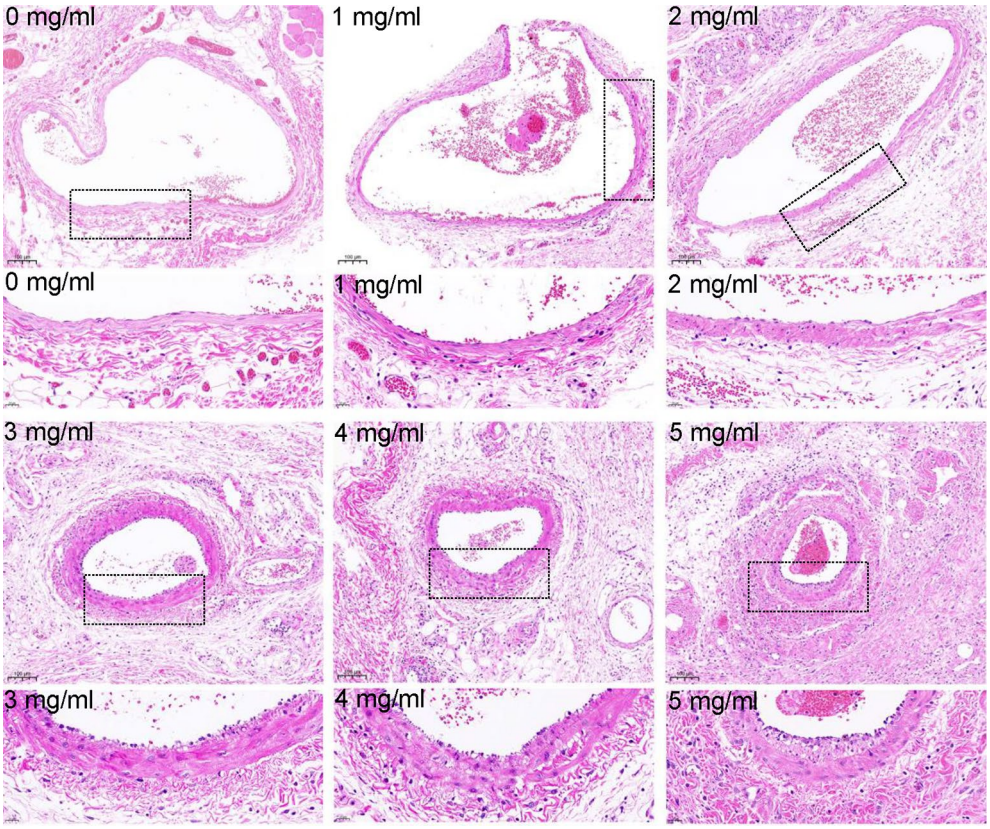


Fig. 2. Representative histopathology images of venous tissues collected from rat hindlimbs stained by hematoxylin-eosin. above, 80×magnification, scale bar = 100 μm; below, 400×magnification, scale bar = 20 μm.

groups. These veins exhibited marked wall thickening, luminal stenosis, and thrombi within the circular venous lumen, indicating progressive dose-dependent venous damage.

Furthermore, venous tissue morphology was assessed using Masson's trichrome staining, as shown in Fig. 3. In venous tissues from the 0 mg/mL and 1 mg/mL vinorelbine groups, endothelial cells rested on the subendothelial connective tissue. Additionally, an internal elastic lamina, composed of aggregated elastic fibers, separated the tunica intima from the tunica media. In contrast, veins injected with higher concentrations of vinorelbine exhibited dose-dependent pathological changes, including wall thickening, luminal stenosis and thrombus. The thickened vein wall with intimal hyperplasia was prominent in the 3, 4, and 5 mg/mL vinorelbine groups, which may result in reduced deformabilit. The neointima was primarily composed of smooth muscle cells interspersed with collagen fibers, while abundant collagen deposition was observed in the tunica adventitia.

Microstructural features in venous tissues

On day 7 post-injection, longitudinal venous tissues from rat hindlimbs were examined by scanning electron microscopy as shown in Fig. 4. In both 0 mg/mL and 1 mg/mL vinorelbine-treated rats, venous tunica intima exhibited a smooth, continuous surface composed of polygonal endothelial cells aligned parallel to the vascular longitudinal axis. Notably, local tunica intima in the 2 mg/mL vinorelbine group adhered to a substantial number of activated platelets. At higher concentrations (3–5 mg/mL), more pronounced dose-dependent mirstructural

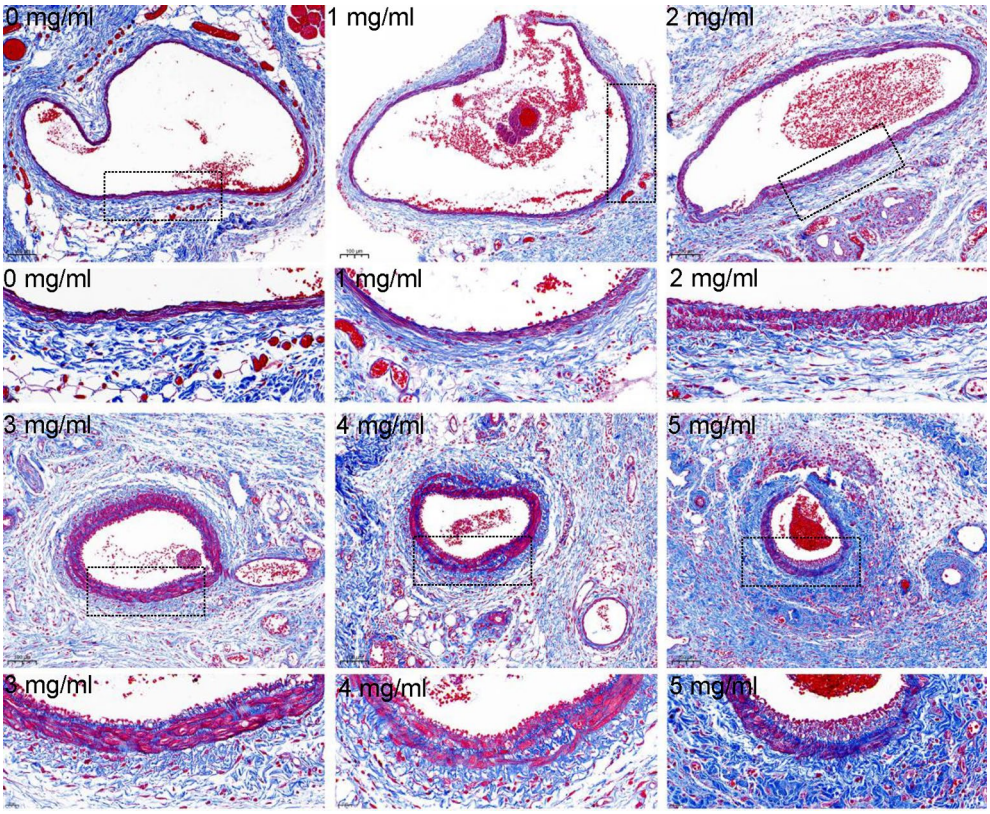


Fig. 3. Representative histopathology images of venous tissues collected from rat hindlimbs stained by masson's trichrome. Collagen fibers were stained blue, muscle fibers and erythrocytes were stained red. above, 80×magnification, scale bar = 100 μm; below, 400×magnification, scale bar = 20 μm.

alterations of lumen surface was observed, characterized by rough with blood cells, densely packed spindle-shaped endothelial cells, and significant accumulation of extracellular matrix.

Further observation of venous transverse sections by transmission electron microscopy as shown in Fig. 5 revealed distinct morphological changes across treatment groups. Venous tissues from 0 mg/mL and low-dose vinorelbine-treated (1–2 mg/mL) rats maintained normal vascular wall architecture, characterized by a tightly aligned monolayer of endothelial cells with prominent nuclei along the luminal surface and an intact basement membrane. In contrast, venous tissues from rats treated with higher vinorelbine concentrations (3 mg/mL, 4 mg/mL, and 5 mg/mL) displayed significant vascular wall thickening. The luminal surface in these groups exhibited crowded arrangements of shrunken endothelial cells intermixed with extracellular matrix.

Discussion

Vinorelbine is a semi-synthetic vinca-alkaloid with a broad spectrum of anti-tumor activity, which has been approved for treating non-small cell lung cancer, breast cancer, ovarian cancer, etc[19]. The recommended dosage for human is 25–30 mg/m^2 and hematological toxicity such as leucopenia is one of dose-limiting adverse reactions. Additionally, the incidence of phlebitis after vinorelbine injection from the peripheral superffcial vein can be as high as 30%[20]. The median lethal dose (LD_{50}) for intravenous administration in rats is 11.2 mg/kg. In our preliminary studies, leucopenia was observed in rats intravenous infused a single dose of 6 mg/kg vinorelbine within 1 day and lasted for at least 7 days. Meanwhile, a significant weight loss also occurred in these rats. In contrast, there were almost no such abnormal events in rats subjected to 3 mg/kg by the same way. So, we designed a protocol of 0.1 mL vinorelbine with a concentration-ascending mode via the dorsalis pedis vein to induce phlebitis in rats. The maximum concentration of vinorelbine used, 5 mg/mL with 0.1 mL, equates to a dose of 1.56 mg/kg in rats, much less than the toxicity dosage.

As mentioned in the background, animal models of chemical phlebitis have primarily been established by intravascular injection vesicants via the marginal ear vein in rabbits or the tail vein in mice. Additionally, rats have been used by injection vinorelbine gel around the tail vein[21], or intradermal injection docetaxel and vinorelbine in lower extremities[22] to induce chemical phlebitis. The rat's dorsal pedal vein with large and superficial vessel runs along the dorsal paw surface, originating from the metatarsal veins and ascending laterally to join the saphenous vein in the hindlimb[23]. So, the distal hindlimb, with superficial venous accessibility and abundant surrounding muscle tissue, provides a more clinically relevant anatomical site for studying phlebitis manifestations and pathogenesis. In the present study, intravascular administered a single 0.1 mL of vinorelbine ranging from 1 mg/mL to 5 mg/mL via the dorsal vein of the hind paw in rats displayed erythema, edema

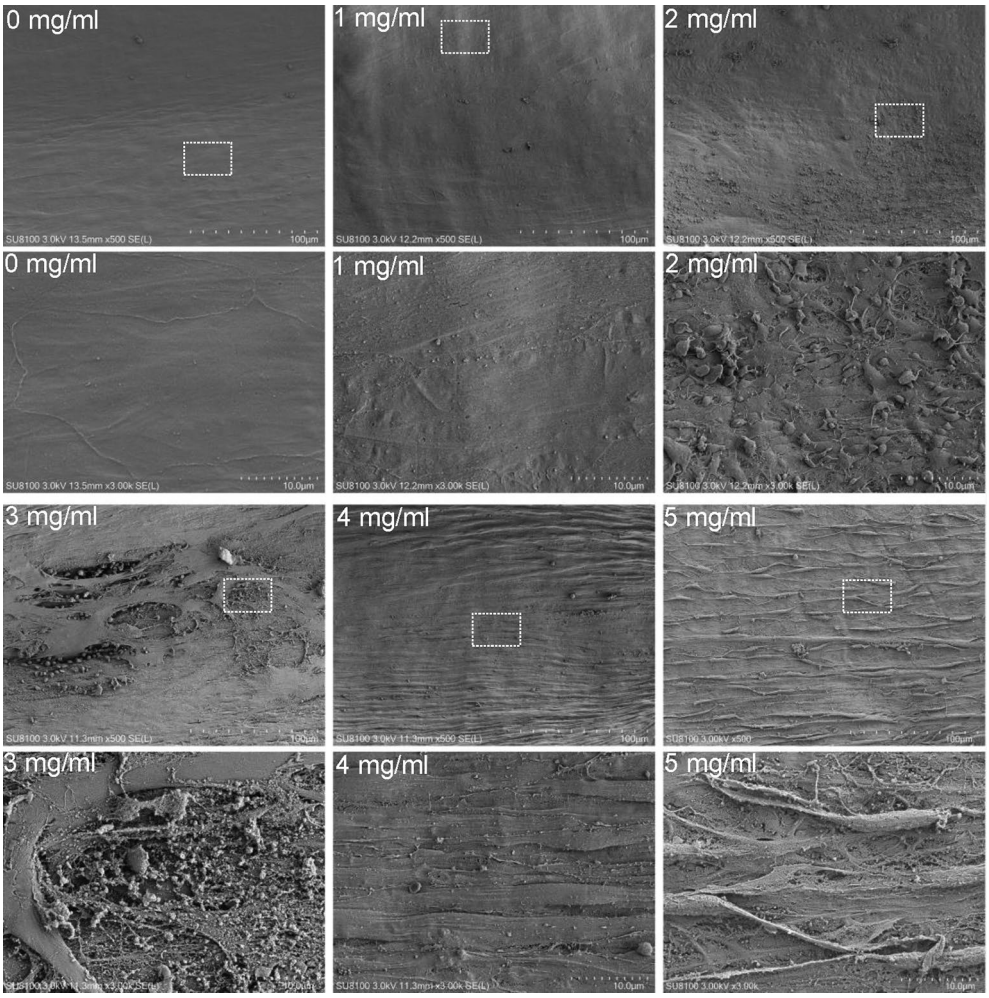


Fig. 4. Representative microstructure images of vascular intima observed by scanning electron microscopy. above, 500×magnification, scale bar = 100 μm; below, 3000×magnification, scale bar = 10 μm.

and pain as early as day 1 post-injection, with symptom severity escalating in a dose-dependent manner. The edema and pain reached peak level on day 3 accompanied by skin ulcer. While these acute symptoms gradually subsided thereafter but followed with induration and streak formation on day 7. By the end of 7 day, all the rats injected vinorelbine in the hindlimb exhibited manifestation of classical phlebitis at concentrations exceeding 3 mg/mL, as assessed by the phlebitis scale. As a whole, rats administered a single 0.1 mL of vinorelbine with a concentration of 3–5 mg/mL via the dorsal vein of the hind paw can induce redness, swelling, pain, cord-like vein and or skin ulceration lasting for at least 7 days.

To date, there has been few studies about the venous pathological features of chemical phlebitis. In fact, it is indeed challenging to obtain lesioned vein specimens from rabbit ears or mouse tails for histological studies, particularly for examining the microstructure of the tunica intima and endothelial cell morphology. Previous study had reported intimal hyperplasia occurred in a porcine thrombosis model induced by electrical injury and partial occlusion of the jugular vein[24]. The dorsal pedal vein in rats is analogous to the superficial veins of the human hand due to its large size and superficial accessibility, making it suitable for microstructural examination. In the present study, the venous tissues in rat injected saline presented flexible and thin wall with classical layers of tunica adventitia, media and intima. Meanwhile, the intima displayed hobnailed endothelium and the large lumen was free of thrombus. Obviously, progressive dose-dependent venous damage was observed in chemical phlebitis rat model by injection vinorelbine via dorsal pedal vein. These leison veins were characterized by vascular wall thickening with intimal hyperplasia, luminal stenosis and thrombus. Meanwhile, the neointima showed predominant smooth muscle cells with interspersed collagen. Vascular endothelial cells form the inner layer of blood vessels where they have a key role in the development and maintenance of the functional circulatory system and provide paracrine support to surrounding non-vascular cells[25]. Endothelial injury is an initial trigger for intimal hyperplasia in vessels, which is a target for developing pharmacological approaches to prevent restenosis[26]. So the microstructure changes in endothelium were observed by electron microscopy[27]. The tunica intima of normal vessles presents a smooth, continuous surface with polygonal endothelial cells aligned parallel to the vascular longitudinal axis. In contrast, the intimal surface of veins exposed to vinorelbine in chemical phlebitis rats was rough with abundant blood cells, even densely packed spindle-shaped endothelial

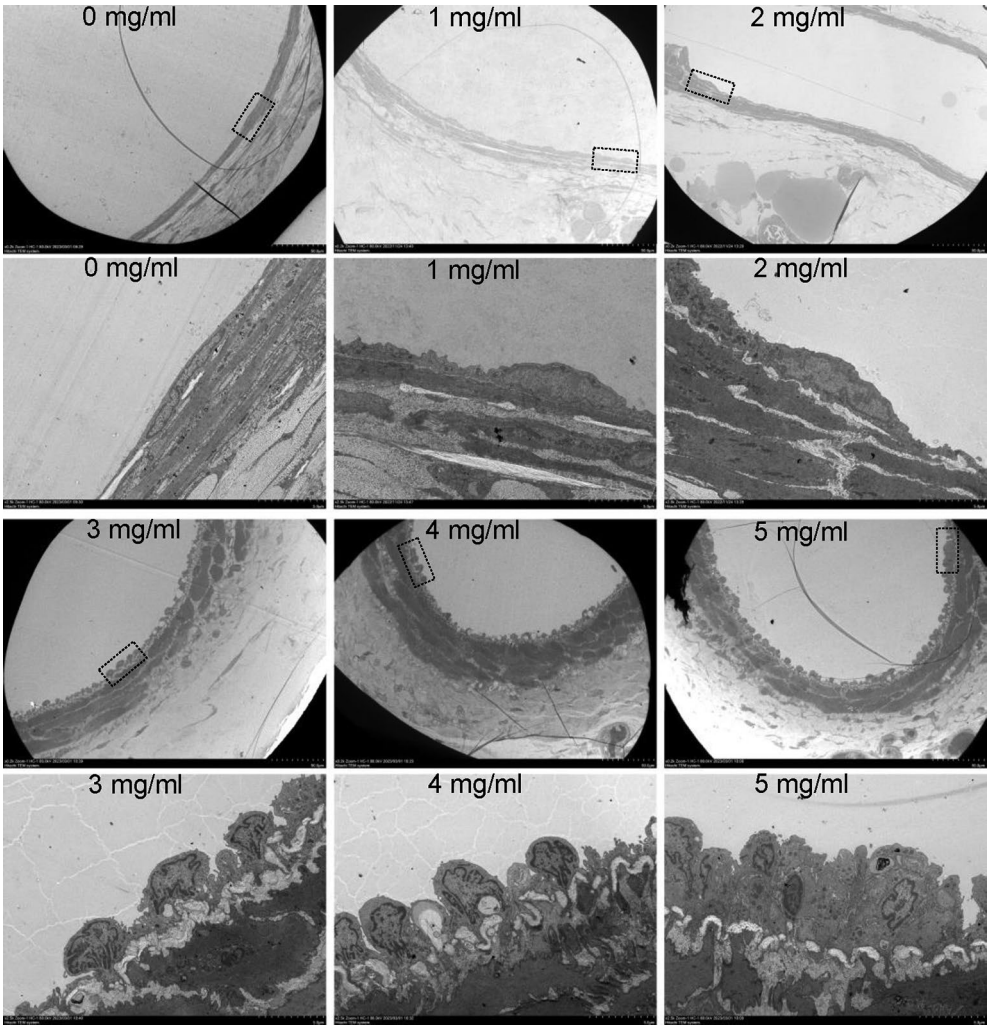


Fig. 5. Representative microstructure images of vascular wall observed by transmission electron microscopy. above, 200×magnification, scale bar = 50 μm; below, 2500×magnification, scale bar = 5 μm.

cells, and significant accumulation of extracellular matrix. These abnormal morphologies are similar to the injuries in human umbilical vein endothelial cells following 1-hour exposure vinorelbine in vitro[28].

The symptomatic and pathological features of chemical phlebitis were characterized in a rat model induced by vinorelbine injection via the dorsal pedal vein. Nevertheless, there are still some limitations. First, the 7-day observation period, while sufficient to capture acute to subacute manifestations such as erythema, edema, pain, and induration, does not reflect the more protracted and complex clinical course seen in patients, which can persist for weeks to months. A longer observation period would be necessary to fully elucidate the natural history of the disease, including its resolution or progression to chronic venous impairment. Second, the underlying molecular mechanisms of vinorelbine-induced phlebitis remain unelucidated. The development of chemical phlebitis entails a complex cascade of events, encompassing endothelial activation, cytokine release, coagulation activation, and inflammatory cell infiltration[29]. Future investigations should, therefore, incorporate analyses of key molecular mediators-such as inflammatory cytokines, adhesion molecules, and pathways implicated in endothelial dysfunction-to delineate the pathogenesis and identify potential therapeutic targets.

Conclusions

This study successfully establishes a novel rat model of chemical phlebitis in a simplicity and good stability method. The hindlimb of rats are suitable for inducing chemical phlebitis by injection vinorelbine with a safety dose via dorsal pedal vein. The symptoms including erythema, pain, edema, palpable cord, and purulent drainage occurred in the hindlimb of rats administered a single 0.1 mL of vinorelbine with 3–5 mg/mL, which may last for at least 7 days. The pathological features in lesion venous tissues were characterized by vascular wall thickening with intimal hyperplasia, luminal stenosis and thrombus. Therefore, future studies should extend the observation period and incorporate molecular investigations to better understand the long-term progression and underlying mechanisms of vinorebitine-induced phlebitis.

Data availability

The datasets used and/or analysed during the current study available from the corresponding author on reasonable request.

Received: 11 August 2025; Accepted: 7 November 2025
Published online: 24 December 2025

References

1. McManus, J. & Huebner, K. Vesicants. *Crit. Care Clin.* **21** (4), 707–718. https://doi.org/10.1016/j.ccc.2005.06.005 (2005). vi.
2. Ballesteros-Peña, S., Fernández-Aedo, I., Vallejo-De la Hoz, G., Tønnesen, J. & Miguelez, C. Identification of potentially irritating intravenous medications. *Enferm. Intensiva (Engl. Ed.)* **33** (3), 132–140. https://doi.org/10.1016/j.enfie.2021.05.003 (2022).
3. Nicotera, R. Phlebitis associated to intravenous/infusional therapy. *Assist. Inferm Ric.* **30** (1), 34–41 (2011).
4. Johnson, J. L. et al. The pharmacist's role in reducing infusion-related phlebitis. *Am. J. Health Syst. Pharm.* **80** (15), 974–983. https://doi.org/10.1093/ajhp/zxad090 (2023).
5. Marshall-McKenna, R. et al. Management of chemotherapy-related arm symptoms in patients with breast cancer. *Cancer Nurs. Pract.* **14**, 22–28 (2015).
6. Heng, S. Y., Yap, R. T. & McGrouther, D. A. Innovative solutions and insights to phlebitis prevention. *Am. J. Med.* **133** (3), 261–264. https://doi.org/10.1016/j.amjmed.2019.07.047 (2020).
7. Annisa, L., Hanifah, S. & Setiani, P. Correlation between the use of vesicant medications and the incidence of phlebitis in pediatric ward. *J. Pharm. Bioallied Sci.* **16** (Suppl 4), S4103–s4106. https://doi.org/10.4103/jpbs.jpbs_1062_24 (2024).
8. Sudhakar, S. et al. Evaluation of chemotherapy infusion and phlebitis among cancer patients: A prospective observational single-center study. *J. Oncol. Pharm. Pract.* **29** (8), 1944–1950. https://doi.org/10.1177/10781552231161517 (2023).
9. Zhang, J. et al. The intervention research on treatment by Xianchen to rabbits model of chemotherapeutic phlebitis. *Acta Cir. Bras.* **31** (8), 549–556. https://doi.org/10.1590/s0102-865020160080000008 (2016).
10. Ge, G. F. et al. Baicalein attenuates vinorelbine-induced vascular endothelial cell injury and chemotherapeutic phlebitis in rabbits. *Toxicol. Appl. Pharmacol.* **318**, 23–32. https://doi.org/10.1016/j.taap.2017.01.013 (2017).
11. Li, G. et al. Experimental study of phlebitis ointment administration in acute superficial thrombophlebitis. *Evid. Based Complement. Alternat. Med.* **2018**, 2983195. https://doi.org/10.1155/2018/2983195 (2018).
12. Fen, Y. et al. The effect of a low-color-temperature-based yellow light source on the prevention of phlebitis induced by chemotherapy. *Biomater. Sci.* **10** (4), 909–914. https://doi.org/10.1039/d1bm01189h (2022).
13. Huang, L. et al. Construction of a rabbit model with Vinorelbine administration via peripherally inserted central catheter and dynamic monitoring of changes in phlebitis and thrombosis. *Exp. Ther. Med.* **23** (3), 212. https://doi.org/10.3892/etm.2022.11135 (2022).
14. Wang, Z. et al. Cimetidine attenuates vinorelbine-induced phlebitis in mice by militating E-selectin expression. *Cancer Chemother. Pharmacol.* **74** (2), 239–247. https://doi.org/10.1007/s00280-014-2487-8 (2014).
15. Liu, P. et al. Chemotherapy-induced phlebitis via the GBP5/NLRP3 inflammasome axis and the therapeutic effect of aescin. *Br. J. Pharmacol.* **180** (8), 1132–1147. https://doi.org/10.1111/bph.16002 (2023).
16. Shejawal, N., Menon, S. & Shailajan, S. A simple, sensitive and accurate method for rat paw volume measurement and its expediency in preclinical animal studies. *Hum. Exp. Toxicol.* **33** (2), 123–129. https://doi.org/10.1177/0960327113482594 (2014).
17. Liu, R. et al. Membrane vesicles from Lactobacillus Johnsonii delay osteoarthritis progression via modulating macrophage glutamine synthetase/mTORC1 axis. *Biomed. Pharmacother.* **165**, 115204. https://doi.org/10.1016/j.biopha.2023.115204 (2023).
18. Gorski, L. A. et al. Infusion therapy standards of practice, 8th Edition. *J. Infus. Nurs.* **44** (1S Suppl 1), S1–S224. https://doi.org/10.1097/nan.0000000000000396 (2021).
19. Gregory, R. K. & Smith, I. E. Vinorelbine–a clinical review. *Br. J. Cancer.* **82** (12), 1907–1913. https://doi.org/10.1054/bjoc.2000.1203 (2000).
20. Yoh, K. et al. High body mass index correlates with increased risk of venous irritation by Vinorelbine infusion. *Jpn J. Clin. Oncol.* **34** (4), 206–209. https://doi.org/10.1093/jjco/hyh029 (2004).
21. Zhu, J. J. et al. Rat injury model of docetaxel extravasation. *Biomed. Rep.* **2** (5), 649–652. https://doi.org/10.3892/br.2014.292 (2014).
22. Zhang, H. et al. N-acetylcysteine attenuates the incidence of phlebitis induced by carbomer/vinorelbine gel. *Heliyon* **9** (11), e21235. https://doi.org/10.1016/j.heliyon.2023.e21235 (2023).
23. Alworth, L. C., Kelly, L. M., Cooper, T. L. & Salyards, G. W. Unassisted blood collection from unanesthetized rats and gerbils. *Lab. Anim. (NY).* **41** (6), 155–156. https://doi.org/10.1038/laban0612-155 (2012).
24. Parsons, R. E. et al. Ultrasonic tissue characterization of experimental venous intimal hyperplasia. *Ultrasound Med. Biol.* **19** (4), 299–308. https://doi.org/10.1016/0301-5629(93)90102-t (1993).
25. Trimm, E. & Red-Horse, K. Vascular endothelial cell development and diversity. *Nat. Rev. Cardiol.* **20** (3), 197–210. https://doi.org/10.1038/s41569-022-00770-1 (2023).
26. Melnik, T., Jordan, O., Corpataux, J. M., Delie, F. & Saucy, F. Pharmacological prevention of intimal hyperplasia: a state-of-the-art review. *Pharmacol. Ther.* **235**, 108157. https://doi.org/10.1016/j.pharmthera.2022.108157 (2022).
27. Tomaiuolo, M., Litvinov, R. I., Weisel, J. W. & Stalker, T. J. Use of electron microscopy to study platelets and thrombi. *Platelets* **31** (5), 580–588. https://doi.org/10.1080/09537104.2020.1763939 (2020).
28. Qian, W. et al. Involvement of Toll-like receptor 4 in vinorelbine-induced vascular endothelial injury. *Exp. Ther. Med.* **10** (1), 62–66. https://doi.org/10.3892/etm.2015.2494 (2015).
29. Zhu, L. L., Wang, Y. H. & Zhou, Q. Progress in research on the mechanisms and interventions of phlebitis from the perspective of vascular endothelial cell and signaling pathway. *J. Inflamm. Res.* **16**, 6469–6481. https://doi.org/10.2147/jir.S450149 (2023).

Acknowledgements

We gratefully appreciate Professor Yaozu Xiang for his insightful comments that greatly improved our manuscript.

Author contributions

Haijie Ji : Conceptualization; formal analysis; investigation; methodology; funding acquisition; writing – original draft; writing – review and editing. Xudong Shi: Data curation; investigation; visualization; writing – original draft; writing – review and editing. Shumin Wang: Investigation; writing – review and editing. Shu Wang: Investigation; writing – review and editing. Dongxue Yan : Investigation; writing – review and editing. Liguo Tong: Investigation; writing – review and editing. Qiming Zhong: Investigation; data curation; writing – review and editing. Mali Feng: Data curation; writing – review and editing. Shulan Hao: Validation; writing – review and

editing. Weiping Li: Conceptualization; formal analysis; methodology; project administration; resources; supervision; writing – review and editing. Xixing Wang: Conceptualization; formal analysis; methodology; project administration; resources; supervision; writing – review and editing.

Funding
This work was funded by the National Natural Science Foundation of China (81973672), the Special Fund for Science and Technology Innovation Team of Shanxi Province (202204051001032), the Fundamental Research Program of Shanxi Province (202203021221291), and the External Expert Studio of Shanxi Province (2025W62).

Competing interests
The authors declare no competing interests.

Ethics statement
The experiments were approved by the Medical Ethics Committee of the Shanxi Academy of Traditional Chinese Medicine (Approval Number: SZYLY2022KY-0302).

Additional information
Correspondence and requests for materials should be addressed to W.L. or X.W.

Reprints and permissions information is available at www.nature.com/reprints.

Publisher's note Springer Nature remains neutral with regard to jurisdictional claims in published maps and institutional affiliations.

Open Access This article is licensed under a Creative Commons Attribution-NonCommercial-NoDerivatives 4.0 International License, which permits any non-commercial use, sharing, distribution and reproduction in any medium or format, as long as you give appropriate credit to the original author(s) and the source, provide a link to the Creative Commons licence, and indicate if you modified the licensed material. You do not have permission under this licence to share adapted material derived from this article or parts of it. The images or other third party material in this article are included in the article's Creative Commons licence, unless indicated otherwise in a credit line to the material. If material is not included in the article's Creative Commons licence and your intended use is not permitted by statutory regulation or exceeds the permitted use, you will need to obtain permission directly from the copyright holder. To view a copy of this licence, visit http://creativecommons.org/licenses/by-nc-nd/4.0/.

© The Author(s) 2025